High frequency A-type pulsators discovered using SuperWASP[*][†]

Daniel L. Holdsworth[1][‡], B. Smalley[1], M. Gillon[2], K. I. Clubb[3], J. Southworth[1],
P. F. L. Maxted[1], D. R. Anderson[1], S. C. C. Barros[4], A. Collier Cameron[5],
L. Delrez[2], F. Faedi[6], C. A. Haswell[7], C. Hellier[1], K. Horne[5], E. Jehin[2],
A. J. Norton[7], D. Pollacco[6], I. Skillen[8], A. M. S. Smith[9], R. G. West[6],
and P. J. Wheatley[6]

[1] *Astrophysics Group, Keele University, Staffordshire, ST5 5BG, United Kingdom*
[2] *Institut d'Astrophysique et de Géophysique, Université de Liège, Allée du 6 Août, 17, Bat. B5C, Liège 1, Belgium*
[3] *Department of Astronomy, University of California, Berkeley, CA 94720-3411, USA*
[4] *Aix-Marseille Universit, CNRS, LAM (Laboratoire d'Astrophysique de Marseille) UMR 7326, 13388 Marseille, France*
[5] *SUPA, School of Physics & Astronomy, University of St. Andrews, North Haugh, Fife, KY16 9SS, UK*
[6] *Department of Physics, University of Warwick, Coventry, CV4 7AL, UK*
[7] *Department of Physical Sciences, The Open University, Walton Hall, Milton Keynes, MK7 6AA, UK*
[8] *Isaac Newton Group of Telescopes, Apartado de Correos 321, 38700 Santa Cruz de la Palma, Tenerife, Spain*
[9] *N. Copernicus Astronomical Centre, Polish Academy of Sciences, Bartycka 18, 00-716 Warsaw, Poland*

15 January 2014

ABSTRACT

We present the results of a survey using the WASP archive to search for high frequency pulsations in F-, A- and B-type stars. Over 1.5 million targets have been searched for pulsations with amplitudes greater than 0.5 millimagnitude. We identify over 350 stars which pulsate with periods less than 30 min. Spectroscopic follow-up of selected targets has enabled us to confirm 10 new rapidly oscillating Ap stars, 13 pulsating Am stars and the fastest known δ Scuti star. We also observe stars which show pulsations in both the high-frequency domain and in the low-frequency δ Scuti range. This work shows the power of the WASP photometric survey to find variable stars with amplitudes well below the nominal photometric precision per observation.

Key words: asteroseismology – stars: chemically peculiar – stars: oscillations – stars: variables: δ Scuti – techniques: photometric – surveys.

1 INTRODUCTION

With the advent of large ground-based photometric surveys (e.g. WASP, Pollacco et al. 2006; HATnet, Bakos et al. 2004; ASAS, Pojmański 1997; OGLE, Udalski et al. 1992) there is a wealth of photometric data on millions of stars. Despite not being the prime science goal, these surveys can be exploited to probe stellar variability across the entire sky (e.g. Norton et al. 2011; Smalley 2013). The ability of these sur-

veys to achieve millimagnitude (mmag) precision provides a vast database in which to search for low-amplitude stellar variability.

The WASP project is a wide-field survey for transiting exoplanets. The project is a two-site campaign: the first instrument is located at the Observatorio del Roque de los Muchachos on La Palma and achieved first light in November 2003, the second is located at the Sutherland Station of the SAAO and achieved first light in December 2005. Each instrument consists of eight 200 mm, f/1.8 Canon telephoto lenses backed by Andor CCDs of 2048×2048 pixels observing ~ 61 deg^2 each through broadband filters covering a wavelength range of $400 - 700$ nm (Pollacco et al. 2006). This set-up enables simultaneous observations of up to 8 fields with a pixel size of $13.7''$. The instruments capture two consecutive 30 s integrations at a given pointing, then move to

the next observable field. Typically, fields are revisited every 10 min.

The images collected are passed through the reduction pipeline, where the data are corrected for primary and secondary extinction, the instrumental colour response and the system zero-point. The atmospheric extinction correction uses a network of stars with a known $(B - V)$ colour to determine the extinction terms, which are then applied to all extracted stars using an assumed colour of G-type stars. This process results in a 'WASP V' magnitude which is comparable to the Tycho-2 V_t passband. The data are also corrected for systematic errors using the SysRem algorithm of Tamuz, Mazeh & Zucker (2005). Aperture photometry is performed at stellar positions provided by the USNO-B1.0 input catalogue (Monet et al. 2003). Stars brighter than $\sim 15^{th}$ magnitude are extracted and provided with a unique WASP ID of the format 1SWASPJ$hhmmss.ss \pm ddmmss.s$. Data are stored in FITS format with labels of the observed field, camera and date of observation. Such a configuration and extended time-base allows the extraction of multiple lightcurves for each object based on either date, field or camera.

To date there are over 428 billion data points in the archive covering over 31 million unique objects. With such a large database of objects it is possible to search for a wide variety of stellar variability.

In this paper we present the results from a survey of the WASP archive in the search of rapidly varying stars. We focus on stars hotter than mid F-type in the region of the Hertzsprung-Russell (HR) diagram where the classical instability strip intersects the main-sequence. In this region we find the classical δ Scuti (δ Sct) pulsators, the non-magnetic metallic-lined (Am) stars, the strongly-magnetic, chemically peculiar, rapidly oscillating Ap (roAp) stars, the metal deficient λ Boötes stars, the γ Doradus (γ Dor) pulsators and the SX Phoenicis variables.

Most of the stars in this region of the HR diagram are δ Sct stars which show normal chemical abundances in their atmospheres. However, at about A8, 50 per cent of the A-type stars are in fact Am stars (Smith 1973). These stars show a discrepancy of at least five spectral subclasses between their hydrogen line spectral class, their Ca K line strength, and their metallic line strengths (Conti 1970). If the differences are less than five subclasses they are designated 'marginal' Am stars (denoted Am:). It was previously thought that the Am stars cannot pulsate with amplitudes greater than 2.0 mmag, if at all (Breger 1970), however a study by Smalley et al. (2011) has shown that ~ 14 per cent of known Am stars pulsate at the mmag level. Their study concluded that the pulsations in Am stars must be laminar so as not to produce sub-cm s^{-1} turbulence which would homogenize the star. The driving mechanism in the Am stars is the opacity (κ) mechanism acting on helium in the He II ionisation zone, resulting in both radial and non-radial pressure modes (p-modes) (see Aerts, Christensen-Dalsgaard & Kurtz 2010).

Rarer than the Am stars are the chemically peculiar Ap stars. Constituting only about 10 per cent of the A-type stars (Wolff 1968), the Ap stars are strongly-magnetic and have over-abundances of rare-earth elements. Around 50 Ap stars are known to be roAp stars (Kurtz 1982). These stars show high-overtone p-mode pulsations in the range of

$5 - 24$ min. The driving mechanism is the same as that for the Am stars, the κ mechanism, but it is acting in the hydrogen ionization zone instead. The pulsational axis in the roAp stars is thought to be aligned with the magnetic field axis rather than the rotational axis, leading to the oblique pulsator model of Kurtz (1982). Due to the strong global magnetic fields, the Ap stars are subject to stratification in their atmospheres, often leading to surface brightness anomalies in the form of chemical spots (Stibbs 1950). These spots can be stable for many decades, allowing for an accurate determination of their rotation period from the lightcurve. The roAp stars provide the best test-bed, beyond the Sun, to study the interactions between pulsations and strong global magnetic fields, as well as testing gravitational settling and radiative levitation theories (e.g. Gautschy & Saio 1998; Balmforth et al. 2001; Kurtz et al. 2011).

Hybrid pulsators, which show both p-mode and gravity (g-) mode pulsations, are also found in this region of the HR diagram. At the base of the instability strip there is an area where the γ Dor stars, g-mode pulsators, overlap with the p-mode δ Sct stars. These objects are of great scientific interest as it becomes possible to probe both the core and atmosphere simultaneously. Observations made with the *Kepler* spacecraft of these hybrid stars (Grigahcène et al 2010; Catanzaro et al. 2011) have shown that these objects are more common than previously thought, with the possibility that nearly all stars in this region of the HR diagram show both γ Dor and δ Sct pulsations (Grigahcène et al 2010).

Finally, we also have the pre-main-sequence A-type stars in this region of the HR diagram. These stars are among the fastest known δ Sct pulsators, with the fastest being HD 34282 with a period of 18 min (Amado et al. 2004). These targets often show multi-mode periodograms, with 'noisy' lightcurves due to dusty circumstellar environments. As a result of this environment many of these objects are heavily reddened.

Previous surveys for pulsations in the A-type stars have targeted objects that were already known to be spectroscopically interesting A stars (e.g. Kochukhov et al. 2013; Paunzen et al. 2012; Smalley et al. 2011). This approach limits the results to specific types of pulsators. However, the approach we have adopted in our study requires no previous knowledge of the targets, except for a rough photometric spectral type. This has allowed us to search for all types of pulsations in F-, A- and B-type stars and will permit the possible discovery of new types, thus the aim of our study is to identify stars which show variability with a period of less than 30 min. This blind survey enables us to approach the search for different types of pulsators in a novel way, opening our results to pulsating Am stars, roAp stars, fast δ Sct stars and pre-main-sequence stars.

2   ARCHIVE SURVEY

2.1   Determining WASP detection limits

Before a full archive survey is conducted, we need to understand the capabilities of the WASP data in detecting pulsations. In order to do this, we employ the micromagnitude (μmag) precision of *Kepler* data.

The *Kepler* mission, launched in March 2009, observed

over 150 000 stars in two cadence modes - the long cadence (LC) mode with an effective exposure time of 30 min was used for the majority of stars, with 512 stars observed in the short cadence (SC) mode with an effective exposure time of 1 min (Gilliland et al. 2010). *Kepler* consisted of an array of 42 CCDs covering 115 $\deg^2$ of sky in the direction of the constellations Cygnus and Lyra. Observations were made through fixed CCD filters covering $423 - 897$ nm (Koch et al. 2010) which is slightly redder than WASP. *Kepler* achieved a photometric precision of up to 84 parts per million (Borucki et al. 2010; Koch et al. 2010) resulting in a large quantity of high cadence data at μmag precision.

Debosscher et al. (2011) have conducted a variability study on the first Quarter of *Kepler* data. We used their results to select 59 737 *Kepler* targets which showed a principal frequency with an amplitude of $\geqslant 0.01$ mmag. Corresponding WASP data were extracted from the archive as long as their $(J - H)$ colour was less than 0.4 so to target G stars and hotter, ensuring we account for reddened objects to maximise our sample size. This resulted in a final sample size of 13 060 stars.

Periodograms for these targets were calculated using the FASPER method of Press et al. (1989, 1992). A small selection of the resulting periodograms were inspected manually where it was found that periodograms suffered greatly from low-frequency noise and a high 'Fourier grass' level – the approximate background level of the periodogram which resembles mown grass – at higher frequencies. Examination of the lightcurves revealed many points which significantly deviated from the mean (Fig. 1 top left). To remove these outliers we have adopted a resistant mean algorithm (Huber 1981) which removes data points from the lightcurve which deviate from the median by more than 4σ. A recalculation of the periodograms resulted in a much smoother periodogram with clearly defined peaks (Fig. 1 top right).

All peaks from each WASP periodogram are compared with the corresponding *Kepler* target data to determine if the pulsation has been detected. We require a maximum deviation of 0.01 d^{-1} between the two data sets to conclude that they agree (the Rayleigh criterion for a typical season of WASP data i.e. $\Delta\nu = 1/\Delta T$, where ΔT is the season duration). We find agreement between 11 188 target stars. Of the non-matches, we determined that if the data set has fewer than 1 000 data points the frequency is not recovered, and if we have a high level of target blending, due to the large WASP pixel sizes, the amplitudes are diluted to below our detection threshold. Of the targets that do match, we are able to conclude that the minimum detection limit is 0.5 mmag.

2.2 Target selection

Using 2MASS colours for stars in the WASP database we select over 1.5 million F-, A- and B-type stars, requiring $(J - H) < 0.25$ (corresponding to F7). We also stipulate that the targets have a USNO magnitude of $14 \leqslant r \leqslant 7$, which are the approximate detection limits of the WASP instruments. Finally we reject stars with fewer than 1 000 data points as we know from Section 2.1 that signals cannot be extracted with so few data.

With our subset of stars we extract each season of data and calculate a periodogram, to a maximum frequency of

300 d^{-1}, as described above. We choose this upper limit to balance computational time with expected detection rate. In all, we calculate over 9 million individual periodograms, indicating an average of 6 seasons per star. To increase the speed of later peak identification we do not store the entire periodogram, only the significant peaks. A peak is deemed significant if it has a S/N > 2.5. To determine the noise level, the periodogram is split into sections of 10 d^{-1} with the mean of each section calculated. The noise level is then taken to be the lowest value calculated. That is to say, the noise is estimated to be half of the 'Fourier grass' level of the most stable section. This value is then used for the entire periodogram. Although not the conventional method to calculate Fourier noise, this method is computationally fast. We have accounted for any over estimates of the noise by lowering the S/N criteria from the widely accepted value of 4 (Breger et al. 1993; Koen 2010). For later analysis of individual targets, for which we use PERIOD04 (Lenz & Breger 2005), we use a threshold S/N of 4.

To identify pulsation candidates in the data with confidence, we require certain criteria to be met. A single object must show a peak at the same frequency in more than one season, within a tolerance of 0.01 d^{-1}. We implement this criterion to reduce the possibility of spurious noise being identified as a true signal. We also consider the window function to eliminate any sampling aliases. Targets which satisfy these criteria have their full periodograms calculated and stored for human inspection.

During this selection process we do not consider the effects of blending or overcrowding of the WASP aperture. Due to the large pixel size of the WASP detectors this can be a common occurrence, with an estimated $\sim 12\%$ of targets suffering $\geqslant 50\%$ dilution. However, at the detection stage, we are solely interested in the detection of variability, with later diagnostics to resolve blends or confusion being conducted to ensure the variability is attributed to the correct target (see Section 4.1.10 for an example).

2.3 Renson & Manfroid catalogue search

To understand the capabilities of the WASP data with regards to finding roAp stars, we conducted an initial test using the catalogue of Renson & Manfroid (2009). All stars identified as Ap were cross-checked with the WASP database, and extracted with the same criteria as in Section 2.2. This amounted to 543 Ap stars. Periodograms were calculated using the aforementioned method, and examined if the above criteria were fulfilled. The automatic search resulted in the extraction of just 1 known roAp star (HD 12932), out of a possible 15 known roAp stars in the subset we searched.

To decipher why only one object was recovered from the WASP data we first consider the spectral response of the WASP instruments. Designed for exoplanet detection, the broad spectral response dilutes the pulsations which are strongest in B-band photometry (Kurtz 1990). Comparing WASP observations of HD 12932 with those in the literature, we see that WASP data suffers an amplitude decrease of ~ 75 per cent. Given the WASP detection threshold is between $0.5 - 1$ mmag, we expect the lower limit in B-band photometry to be between $2 - 4$ mmag, thus accounting for the non-detection of 10 targets.
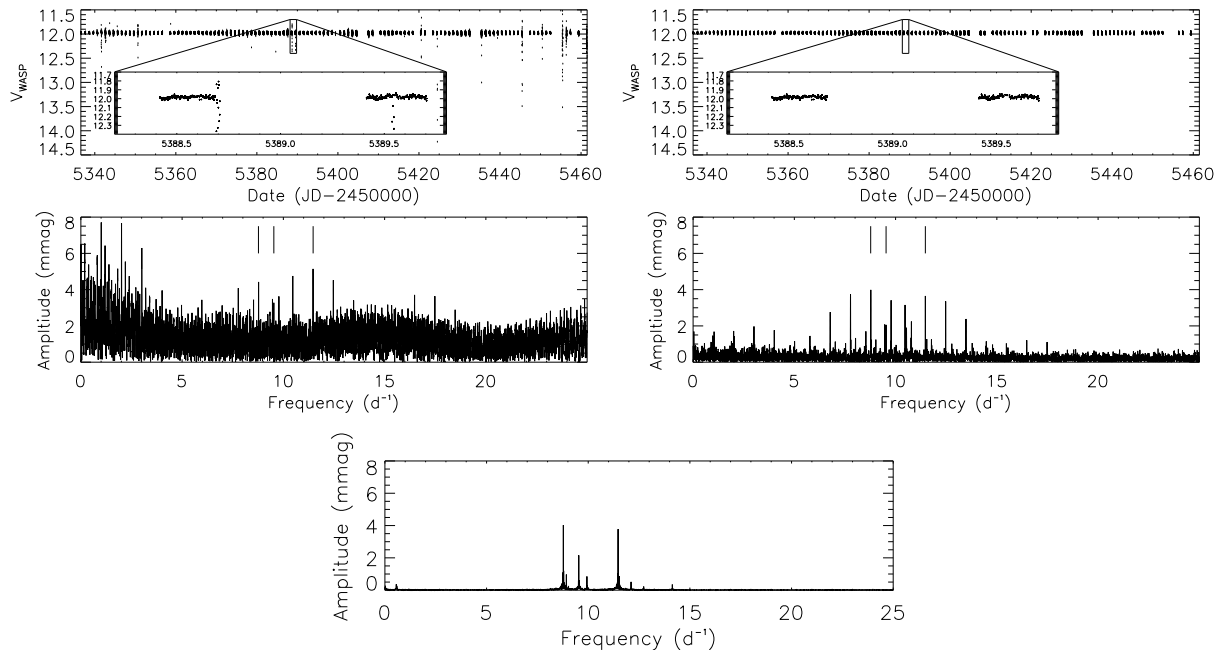
Figure 1. A comparison of the raw (top left), 14 659 data points, and cut (top right), 13 970 data points, lightcurves and corresponding periodograms for 1SWASPJ192444.63 + 490052.2. The much cleaner lightcurve shown in the top right plot results in a clean periodogram, with a Fourier grass level of about 0.5 mmag, which clearly shows the principal frequency at 8.77 d^{-1}, a secondary peak at 11.47 d^{-1} and a third peak at 9.53 d^{-1}. The top left periodogram does not identify the principal frequency correctly due to high-amplitude, low-frequency noise; the Fourier grass level is about 2.5 mmag with the amplitudes of the peaks are also much higher here too. It is clear that the use of resistant mean clipping greatly enhances detection probability. The three pulsation frequencies are marked with vertical lines. The bottom plot shows the corresponding *Kepler* data of KIC 11295729, the same star as 1SWASPJ192444.63 + 490052.2.

We further investigate why we detect no pulsations for the remaining 4 targets by calculating for each season of data the weighted reduced-χ^2 (Bevington 1969) which aims to characterize the lightcurve by accounting for the number of data points and the scatter in the lightcurve i.e.

$$\chi^2/n = \frac{\Sigma((\text{mag} - \text{median}(\text{mag}))/\sigma)^2}{(n-1)}.$$

With this taken into account, it becomes more clear why we do not detect the roAp stars with amplitudes above our expected amplitude threshold. For the four non-detected targets above the threshold, the χ^2/n value suggests the data are not of high enough quality to consistently detect pulsations.

This suggests we will only detect a small fraction of the roAp stars that exist in the WASP database. The main reason for the lack of detections of the known targets is the colour response of the WASP instruments. For the target that was automatically extracted, the amplitude dilution of 75 per cent indicates that we will only observe the highest amplitude pulsators.

Of the 543 Ap stars we studied, we detected no new roAp stars amongst the sample. We are, of course, limited by our threshold of 0.5 mmag which provides an upper limit on any pulsations in the WASP *V*-band photometry.

3   CANDIDATE TARGETS

Of the 1.5 million F-, A- and B-type stars extracted from the WASP archive, we find 375 stars which show variations on the order of 30 min or less which are present in two or more seasons of observations. Of these 375 targets, we obtained spectral follow-up for 37 stars. The targets were selected for follow-up based on their frequency and amplitude of pulsation. Focusing initially on the objects whose periodograms look like that of the rare roAp stars, then moving to lower frequencies and periodograms which show a more complex pulsation spectrum. In Table 2 we present photometric information on the 37 stars for which we obtained spectra.

3.1   Spectroscopy

To obtain spectra for our candidate stars, we make use of the Intermediate dispersion Spectrograph and Imaging System (ISIS) mounted on the 4.2-m William Herschel Telescope (WHT) in service mode for our northern targets, and the Robert Stobie Spectrograph (RSS) mounted on the 10-m Southern African Large Telescope (SALT) to observe our southern targets. We require only low resolution classification spectra for our targets, achieving a spectral resolution of ~ 5000 for SALT/RSS observations and ~ 2000 for WHT/ISIS observations. In addition, two objects were observed with the Hamilton Echelle Spectrograph (HamSpec; Vogt 1987) on the Shane 3-m telescope at Lick Observatory, achieving a resolution of $R \sim 37\,000$.

Table 1. Renson and WASP coincident roAp stars. Columns $9-16$ are a measure of the quality of the WASP data for each season.

HD	Literature Data			WASP Data											
	Mag (B)	ν (d^{-1})	ΔB (mmag)	Mag (V_{WASP})	ν (d^{-1})	ΔV (mmag)	$N°$ of Seasons	χ^2/n							
6532	8.60	202.82	5	8.38	–	–	2	42.43	2.33						
9289	9.63	137.14	3.5	9.42	–	–	4	7.46	14.93	3.73	2.66				
12098	8.46	189.22	3	8.23	–	–	1	1.82							
12932	10.56	124.14	4	10.28	124.10	1.03	5	1.18	1.07	0.99	1.17	0.97			
84041	9.74	96.00	6	9.25	–	–	5	44.65	9.52	3.95	7.76	6.29			
99563	8.90	134.58	10	8.50	–	–	4	12.28	204.96	11.33	2.65				
101065	8.73	119.01	13	8.27	–	–	2	2.44	5.65						
119027	10.41	165.52	2	10.19	–	–	4	1.58	1.27	8.69	1.79				
122970	8.70	129.73	2	8.33	–	–	4	2.89	4.60	6.95	3.90				
185256	10.37	141.18	3	10.10	–	–	7	3.77	2.18	0.934	1.47	2.91	1.43	37.82	
193756	9.56	110.77	1.5	9.27	–	–	5	3.29	0.95	1.82	4.25	3.10			
196470	10.14	133.33	0.7	9.84	–	–	6	3.02	4.10	3.53	4.91	2.58	4.48		
203932	9.10	244.07	2	8.92	–	–	4	23.25	3.80	0.66	17.62				
213637	10.05	125.22	1.5	9.73	–	–	8	1.52	1.63	1.53	2.06	1.52	1.42	0.89	1.36
218495	9.62	194.59	1	9.43	–	–	4	7.95	6.41	5.62	7.81				

Table 2. Photometric data for the 37 high-frequency WASP pulsators for which spectra were obtained. Column 8 is the number of data points in the WASP archive for that object after applying our cleaning routine, column 9 is the principal pulsation frequency above 50 d^{-1}, and column 10 is the pulsational amplitude in the WASP data.

Abbreviated ID	Other ID	R.A. J2000	Dec J2000	V	$(J-H)$	$N°$ of Seasons	npts	ν_{osc} (d^{-1})	Amp (mmag)
J0004	HD 225186	00:04:15.12	-17:25:29.6	9.05	0.152	4	13814	60.08	3.40
J0008	TYC 4-562-1	00:08:30.50	$+04$:28:18.2	10.16	0.087	3	23076	150.26	0.76
J0026[a]	TYC 2269-996-1	00:26:04.18	$+34$:47:32.9	10.04	0.232	3	13037	79.13	2.05
J0051	TYC 5270-1900-1	00:51:07.36	-11:08:31.9	11.52	0.059	3	21913	58.04	4.77
J0206[b]	HD 12932	02:06:15.80	-19:07:26.2	10.17	0.105	4	15269	124.10	1.38
J0353	HD 24355	03:53:23.09	$+25$:38:33.3	9.65	0.054	3	7951	224.31	1.65
J0410	HD 26400	04:10:45.78	$+07$:17:17.2	9.54	0.017	3	28629	68.22	2.70
J0429	HD 28548	04:29:27.24	-15:01:51.1	9.22	0.038	2	22195	65.65	4.41
J0629	HD 258048	06:29:56.85	$+32$:24:46.9	10.52	0.239	3	15343	169.54	1.49
J0651	TYC 8912-1407-1	06:51:42.17	-63:25:49.6	11.51	0.062	3	36597	132.38	0.79
J0855	TYC 2488-1241-1	08:55:22.22	$+32$:42:36.3	10.80	0.014	3	13203	197.27	1.40
J1110	HD 97127	11:10:53.91	$+17$:03:47.5	9.43	0.172	3	11184	106.61	0.66
J1215	HD 106563	12:15:28.17	-11:24:41.3	10.55	-0.021	3	16354	65.46	1.48
J1250	TYC 297-328-1	12:50:56.15	$+05$:32:12.9	11.25	0.168	4	22902	68.99	4.30
J1403	HD 122570	14:03:41.51	-40:51:08.9	10.41	0.079	4	19613	99.12	1.27
J1430	TYC 2553-480-1	14:30:49.64	$+31$:47:55.1	11.56	0.094	3	21181	235.54	1.06
J1625	HD 147911	16:25:24.10	-21:41:18.6	9.17	0.186	5	21514	68.52	6.37
J1640	2MASS J16400299-0737293	16:40:02.99	-07:37:29.7	12.67	0.150	2	14511	151.93	3.52
J1648	TYC 2062-1188-1	16:48:36.99	$+25$:15:48.6	9.98	0.123	5	43024	105.12	0.60
J1757	TYC 2612-1843-1	17:57:26.48	$+32$:25:23.7	11.58	0.173	5	35794	63.71	2.46
J1758	2MASS J17584421+3458339	17:58:44.20	$+34$:58:33.9	12.93	0.11	5	74131	71.28	2.49
J1844	TYC 3130-2480-1	18:44:12.27	$+43$:17:51.9	11.25	0.072	5	39389	181.73	1.45
J1917	TYC 7926-99-1	19:17:33.42	-42:42:07.3	11.18	0.144	3	12120	164.47	1.85
J1940	2MASS J19400781-4420093	19:40:07.81	-44:20:09.2	13.02	0.066	5	25071	176.39	4.16
J1951	2MASS J19512756-6446247	19:51:27.55	-64:46:24.5	13.26	-0.010	4	28567	58.43	4.29
J2022	TYC 9311-73-1	20:22:36.50	-70:11:00.2	12.77	0.022	4	27249	62.54	3.30
J2026	TYC 5762-828-1	20:26:42.62	-11:52:45.1	11.80	0.232	4	15957	212.66	1.62
J2029	HD 195061	20:29:33.21	-18:13:12.2	9.81	0.072	6	24743	28.86	2.50
J2054	TYC 525-2319-1	20:54:19.84	$+07$:13:11.0	9.94	0.020	5	31892	104.86	1.10
J2155	2MASS J21553126+0849170	21:55:31.26	$+08$:49:17.0	12.83	0.214	4	29563	61.34	6.38
J2241	TYC 3218-888-2	22:41:54.21	$+40$:30:39.1	11.45	0.063	3	10389	75.54	3.32
J2254	TYC 569-353-1	22:54:34.21	$+00$:52:46.3	12.72	0.163	3	33997	52.59	5.06
J2255	TYC 6390-339-1	22:55:20.44	-18:36:35.3	11.95	-0.029	4	17232	66.96	2.68
J2305	TYC 9131-119-1	23:05:45.31	-67:19:03.0	11.43	-0.019	2	16265	92.75	1.61
J2313	TYC 577-322-1	23:13:26.32	$+02$:27:49.5	10.72	0.109	3	24001	60.42	5.97
J2345	2MASS J23455445-3932085	23:45:54.44	-39:32:08.2	13.60	0.006	2	11594	60.47	20.33

[a] This target is classed as one star in the WASP archive but is in fact a visual binary.
[b] This is a known roAp star included for comparison.

All spectra have been extracted from their FITS images and have been flat-field corrected, de-biased, cleaned of cosmic-rays and have had wavelength calibrations applied. Tools from the STARLINK project[1] were used to perform these tasks, with the exception of the HamSpec spectra, which were reduced using routines written in IDL. Finally, the spectra were intensity rectified using the UCLSYN spectral synthesis package (Smalley, Smith & Dworetsky 2001).

To determine the stellar temperatures from the spectra we used UCLSYN, setting $\log g$ to a constant 4.0 and synthesised the Balmer lines. Due to the low resolution classification spectra, we are only able to attain the temperatures to within ± 200 K. We estimate the S/N for each spectrum using the DER_SNR code of Stoehr et al. (2008). The spectral types of the stars were determined via comparison with MK Standard stars using the method of Gray & Corbally (2009). We present the spectroscopic information and results in Table 3.

3.2 Stellar temperatures from spectral energy distributions

Effective temperatures can be determined from the stellar spectral energy distribution (SED). For our target stars these were constructed from literature photometry, using 2MASS (Sktrutskie et al. 2006), DENIS (Fouqué et al. 2000), Tycho B and V magnitudes (Høg et al. 1997), USNO-B1 R magnitudes (Monet et al. 2003), TASS V and I magnitudes (Droege et al. 2006) CMC14 r' magnitudes (Evans, Irwin & Helmer 2002) as available.

The stellar $T_{\rm eff}$ values were determined by fitting solar-composition Kurucz (1993) model fluxes to the de-reddening SEDs. The model fluxes were convolved with photometric filter response functions. A weighted Levenberg-Marquardt non-linear least-squares fitting procedure was used to find the solution that minimized the difference between the observed and model fluxes. Since $\log g$ is poorly constrained by our SEDs, we fixed $\log g = 4.0$ for all the fits. Stellar energy distributions can be significantly affected by interstellar reddening. However, in the absence of measured reddening values, we have assumed $E(B - V) = 0.02 \pm 0.02$ in our fitting. The uncertainties in $T_{\rm eff}$ includes the formal least-squares error and adopted uncertainties in $E(B-V)$ of ± 0.02 and $\log g$ of ± 0.5 added in quadrature. We present the SED derived $T_{\rm eff}$ for our spectroscopically observed targets in Table 3.

4 RESULTS

4.1 New roAp stars

We present here the 10 new roAp stars discovered in the SuperWASP archive. Some objects show a low frequency signature in their periodogram which is attributed to rotational modulation. We present both the low frequency periodograms and the phase folded lightcurves alongside a discussion of each object, with the details of the modulations shown in Table 4. The periodograms indicate the frequency (ν) on which the data are folded, as well as labels of other

Table 4. Rotationally modulated lightcurve data for the newly detected roAp stars.

ID	ν_{rot} (d^{-1})	Period (d)	Amp (mmag)	FAP
J0353	0.0717	13.95	6.37	<0.001
J0855	0.3234	3.09	2.55	0.096
J1640	0.2722	3.67	4.17	0.003
J1844	0.0495	20.20	7.65	0.000
J1940	0.1044	9.58	5.87	0.017
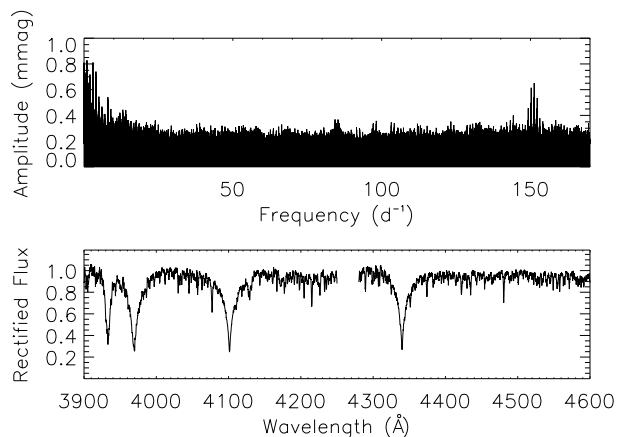
Figure 2. Periodogram and SALT/RSS spectrum of J0008. The low frequency peaks in the periodogram are due to noise.

prominent peaks. In this frequency range the periodograms show the reflection of the -1 d^{-1} aliases, labelled as $-\nu$, which must not be confused with the true peak. Each periodogram is calculated with a single season of WASP data for clarity (the peaks are also present in all other data sets for each target). The solid line on each phase plot represents the harmonic fit. The false-alarm probability (FAP) is calculated using the method of Maxted et al. (2011).

4.1.1 J0008

J0008 shows roAp pulsations at 150.26 d^{-1} with an amplitude of 0.76 mmag (Fig. 2 top). WASP has observed the target for three consecutive seasons with slight discrepancies in the pulsation frequency which is attributed to the 1-d aliases. The spectrum obtained for this star (Fig. 2 bottom) has been classified as A9p, with strong enhancements of Sr II and Eu II. The spectrum confirms this to be a new roAp star.

The pulsations in J0008 are similar to those in HD 119027, which pulsates at 165.52 d^{-1} with an amplitude in the blue of 2.0 mmag (Martinez & Kurtz 1994). HD 119027 is a hotter star, classified as A3p SrEu(Cr), and is also known to show amplitude modulation as a result of closely spaced frequencies.

4.1.2 J0353

The star J0353 displays pulsations at about 224 d^{-1} with an amplitude of 1.65 mmag as well as a low-frequency variation

Table 3. Spectroscopic information on the 37 targets for which we obtained follow-up spectra.

ID	Telescope/ Instrument	Exposure (s)	Observation Date	S/N	Balmer $T_{\rm eff}$ (K)	SED $T_{\rm eff}$ (K)	Spectral Type
J0004	SALT/RSS	15	2012-05-31	180	7900	7518 ± 377	A5
J0008	SALT/RSS	99	2013-06-15	60	7300	7484 ± 336	A9p SrEu(Cr)
J0026S[a]	WHT/ISIS	30	2011-11-22	100	6650	6100 ± 318	F4
J0026P	WHT/ISIS	30	2011-11-22	115	8100		A2m
J0051	SALT/RSS	200	2013-06-06	50	7850	8144 ± 479	A6
J0206	WHT/ISIS	30	2011-11-22	70	7600	7310 ± 318	A4p
J0353	WHT/ISIS	15	2012-10-24	50	8250	7417 ± 331	A5p SrEu
J0410	WHT/ISIS	20	2011-11-22	125	8150	7712 ± 346	A3m:
J0429	WHT/ISIS	15	2013-10-24	120	8200	8770 ± 334	A2m
J0629	WHT/ISIS	40	2012-10-24	40	6600	6211 ± 281	F4p EuCr(Sr)
J0651	SALT/RSS	1300	2012-09-11	70	7400	7843 ± 491	F0p SrEu(Cr)
J0855	WHT/ISIS	50	2011-11-22	80	7800	8287 ± 475	A6p SrEu
J1110	WHT/ISIS	15	2012-12-25	55	6300	6707 ± 294	F3p SrEu(Cr)
J1215	WHT/ISIS	40	2012-12-25	70	8100	8437 ± 412	A3m:
J1250	WHT/ISIS	100	2012-12-25	100	8300	7099 ± 370	A4m
J1403	SALT/RSS	500	2012-05-08	140	7550	7500 ± 350	A9
J1430	WHT/ISIS	100	2012-12-25	85	7100	7479 ± 366	A9p SrEu
J1625	SALT/RSS	230	2012-05-08	235	8200	6147 ± 272	A1m
J1640	{ WHT/ISIS	1200	2013-02-01	95	7400	6282 ± 314	A8p SrEu
	{ SALT/RSS	600	2013-03-22	75	7400		A8p SrEu
J1648	WHT/ISIS	200	2013-02-01	80	7100	6939 ± 307	F0
J1757	WHT/ISIS	600	2013-02-01	105	7900	7425 ± 377	A7m:
J1758	WHT/ISIS	1200	2013-02-01	110	7700	7260 ± 480	A7m:
J1844	Shane/HamSpec	1800	2012-07-24	40	7000	8043 ± 435	A7p EuCr
J1917	SALT/RSS	249	2013-04-22	100	7800	6989 ± 293	A7m
J1940	SALT/RSS	759	2012-11-03	20	6900	7623 ± 411	F2(p Cr)
J1951	SALT/RSS	900	2013-04-25	75	8100	8076 ± 438	A5
J2022	SALT/RSS	500	2013-04-25	85	8200	7973 ± 507	A4m
J2026	WHT/ISIS	150	2013-04-25	60	6000	6528 ± 433	F8
J2029	SALT/RSS	25	2013-04-27	40	8000	7754 ± 339	A4m
J2054	Shane/HamSpec	1800	2012-07-24	60	7000	8372 ± 438	A3m:
J2155	SALT/RSS	800	2013-06-07	50	8100	6681 ± 555	A3
J2241	WHT/ISIS	100	2012-10-25	70	8100	7771 ± 391	A3m
J2254	SALT/RSS	600	2013-06-17	55	8150	7059 ± 450	A4
J2255	SALT/RSS	250	2013-05-13	50	8200	8564 ± 627	A3
J2305	SALT/RSS	139	2012-11-04	35	8050	8146 ± 374	A5m:
J2313	SALT/RSS	90	2013-06-19	65	8000	7794 ± 376	A5
J2345	SALT/RSS	1250	2013-06-07	75	9700	9772 ± 964	A3

[a]We identify this target as a spectroscopic binary, with a radial velocity shift of 172 ± 21 km s^{-1}.

corresponding to 13.95 d (Fig. 3 & Fig. 4). The spectrum of this star is classified as A5p with an enhancement of Sr II and Eu II, confirming it as a new roAp star.

Similar to J0353, HR 1217 shows pulsations at about the same frequency (232.26 d^{-1}; Kurtz 1981) and is classified as an A9p SrEu(Cr) star. The rotation period of HR 1217 has been discussed at length in the literature, recently Rusomarov et al. (2013) present a period of 12.45812 d derived from 81 longitudinal magnetic field data points spanning over 4 decades. Balona & Zima (2002) present spectra of HR 1217 which show a core-wing anomaly in the H$_\alpha$ line, a feature which we also note in our ISIS red-arm spectrum.

4.1.3 J0629

J0629 has pulsations at 169.54 d^{-1} with an amplitude of 1.49 mmag (Fig. 5 top). The spectrum (Fig. 5 bottom) shows strong over-abundances of Sr II, Cr II and Eu II. The pho-

tometric observations give no indication of rotational modulation. We classify the star as F4p.

Through both Balmer line analysis and SED fitting, we conclude that J0629 is a very cool Ap star with a $T_{\rm eff}$ similar to the roAp star HD 213637 (6400 K; Kochukhov 2003), and thus placing J0629 amongst the coolest roAp stars.

4.1.4 J0651

We classify J0651 as an F0p star whose spectrum shows a strong over-abundance of Sr II at $\lambda\lambda$ 4077 & 4216 (Fig. 6). We also see enhanced features of Eu II at $\lambda\lambda$ 4128 & 4205 and Cr II at λ 4111. Our photometry shows pulsations at 132.38 d^{-1} (Fig. 6), with no clear indications of rotational modulation in the lightcurve.

In the literature we find a very similar roAp star to J0651. Pulsating at a frequency of 137.17 d^{-1} with an amplitude in the blue of 3.5 mmag, HD 9289 is an Ap SrEu star (Kurtz & Martinez 1993). Elkin, Kurtz & Mathys
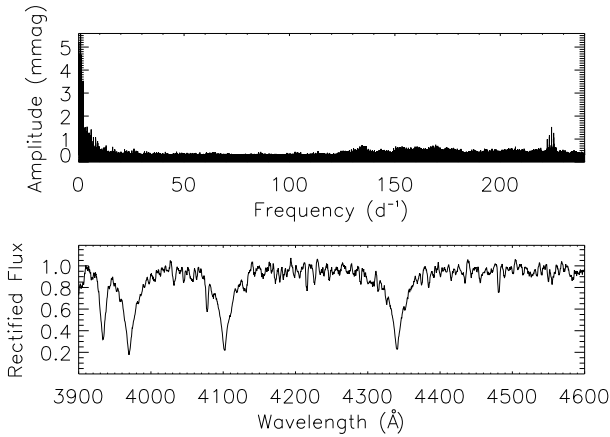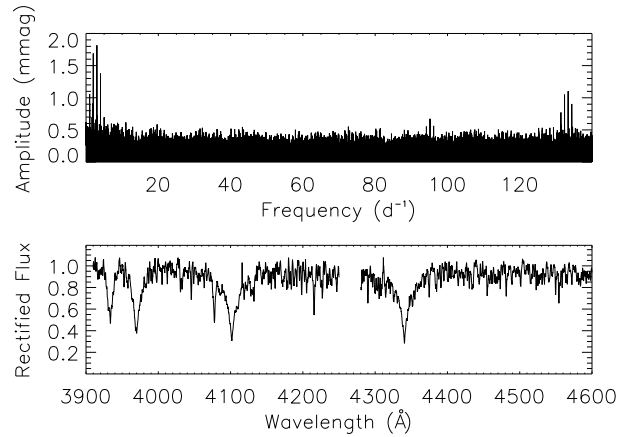
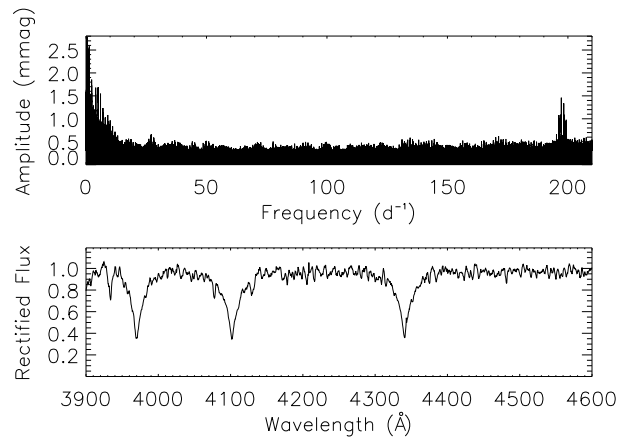**Figure 3.** Periodogram and WHT/ISIS spectrum of J0353.
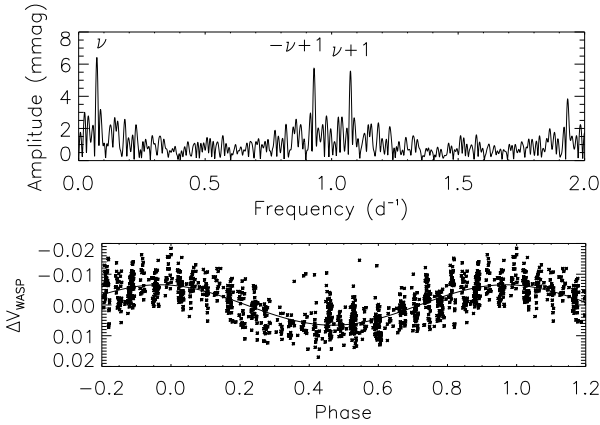
Figure 4. Low frequency periodogram and phase folded WASP lightcurve for J0353. The data are folded on a period of 13.95 d, and shown in phase bins of 0.001. The labelled peaks are the true frequency (ν) and the positive and negative aliases.
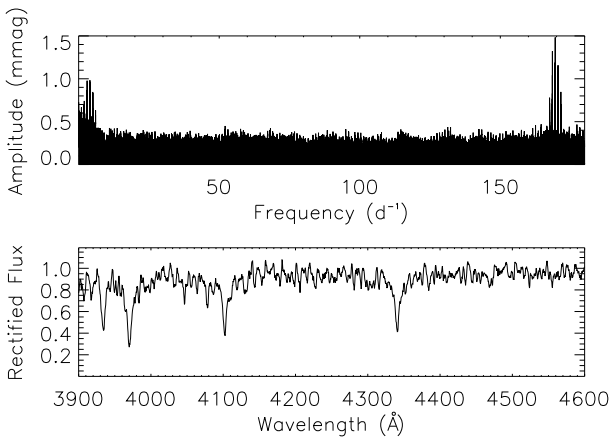
Figure 5. Periodogram and WHT/ISIS spectrum of J0629. The low frequency peaks in the periodogram are due to 1-d aliasing.
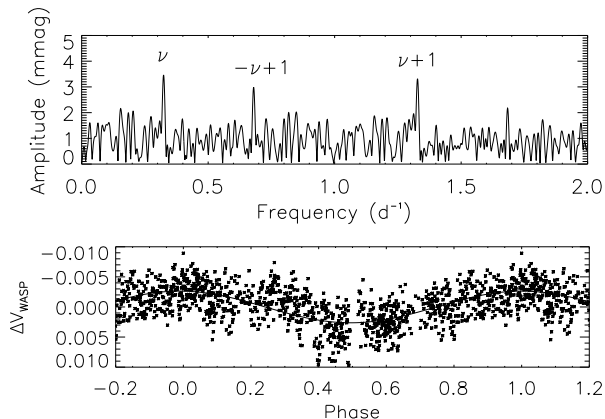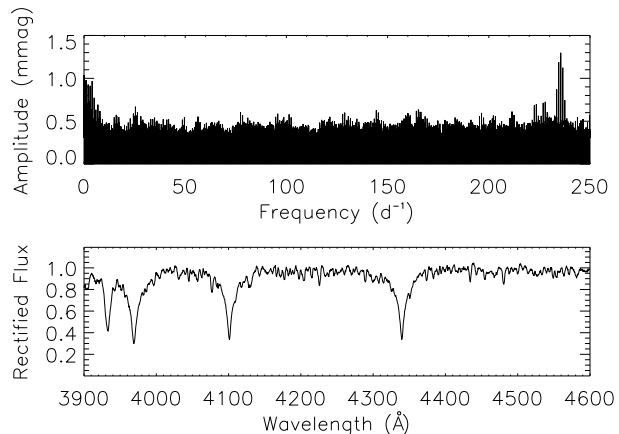

Figure 6. Periodogram and SALT/RSS spectrum of J0651. The low frequency peaks in the periodogram are due to 1-d aliasing.

Figure 7. Periodogram and WHT/ISIS spectrum of J0855.

(2008) present photometric and spectroscopic $T_{\rm eff}$ values for HD 9289, deriving 7700 and 8000 K respectively, which are similar to those we obtain for J0651.

4.1.5   J0855

J0855 shows rapid pulsations at 197.27 d^{-1} with an amplitude of 1.4 mmag (Fig. 7). Balmer line fitting gives a $T_{\rm eff}$ of 7800 K, and a spectral type of A6p when compared to MK standards. The spectrum also shows an over-abundance of Eu II at $\lambda\lambda$ 4205 & 4128, with weak Ca K and Ca I at $\lambda4266$ (Fig. 7). As well as the high-frequency pulsation, the periodogram shows a low-frequency signature with a period of 3 d (Fig. 8).

Our temperatures derived for J0855 vary greatly between methods, however the SED method is very poorly constrained for this target as indicated by the error bar. Assuming a $T_{\rm eff}$ of that derived through Balmer line fitting, J0855 is almost identical to the known roAp star HD 190290 (Martinez & Kurtz 1990). The pulsations of the two are at the same frequency, with J0855 showing a larger undiluted amplitude. The ISIS red arm spectrum also shows a core-wing anomaly in the H$_\alpha$ line.

Figure 8. Low frequency periodogram and phased folded lightcurve of J0855 folded on a period of 3.09 d and shown in phase bins of 0.001. Thee labelled peaks are the true frequency (ν) and the positive and negative aliases.
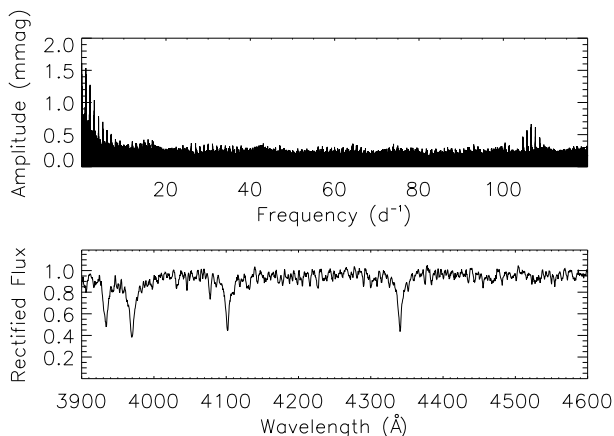
Figure 9. Periodogram and WHT/ISIS spectrum star J1110. The low frequency peaks in the periodogram are due to 1-d aliasing.

4.1.6 J1110

J1110 exhibits low amplitude pulsations at 106 d^{-1} (Fig. 9). We classify the spectrum as a cool F3p star with a $T_{\rm eff}$ measured from the Balmer lines of 6500 K. The spectrum shows a slight over-abundance of Eu II at $\lambda\lambda$ 4128 & 4205, and a marginal over-abundance of Sr II (Fig. 9). We also note the weak Ca I K and λ4266 lines which may be due to stratification in the atmosphere.

J1110 has the lowest pulsation frequency of our roAp stars and is also the coolest, as derived from the Balmer lines. J1110 is similar in amplitude and frequency to HD 193756. However, HD 193756 is classified as A9 with a temperature of 7500 K derived from its H$_\alpha$ profile (Elkin et al. 2008).

4.1.7 J1430

Pulsating at a frequency of 235.5 d^{-1} with an amplitude of 1.06 mmag (Fig. 10), we classify J1430 as an A9p star with an effective temperature of 7100 K derived from the Balmer lines. The spectrum shows an over-abundance of Eu II (Fig.

Figure 10. Periodogram and WHT/ISIS spectrum of J1430. The low frequency peaks in the periodogram are due to noise.
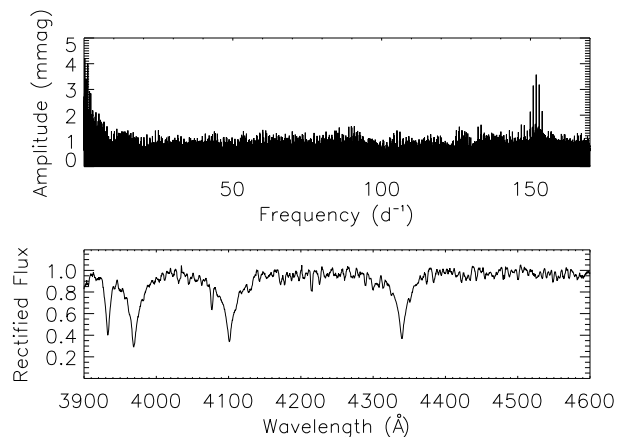
Figure 11. Periodogram and WHT/ISIS spectrum of J1640.

10). J1430 is the fastest roAp star we have found in the WASP archive, and is third fastest of all the roAp stars.

HD 86181 is a similar object to J1430 in both pulsations and temperature. HD 86181 has a $T_{\rm eff}$ of 7900 K (Balmforth et al. 2001), but is classified as only having an over-abundance of Sr. The H$_\alpha$ line profile of J1430 indicates the presence of a core-wing anomaly.

4.1.8 J1640

WASP photometry shows J1640 to pulsate at 151.93 d^{-1} with an amplitude of about 3.5 mmag (Fig. 11). The classification spectrum shows over-abundances of both Sr II and Eu II allowing us to classify this star as A8p (Fig. 11). We also detect in the photometry a signature with a period of 3.67 d, most likely due to the rotation of the star (Fig. 12).

We obtained two spectra of this target using two different instruments. The separate analysis of both spectra resulted in the same classification and $T_{\rm eff}$. There are no known roAp stars which exhibit a similar pulsation spectrum as J1640, in the sense that J1640 is exhibits pulsations of 3.52 mmag in our diluted photometry, making it one of the highest amplitude pulsators.
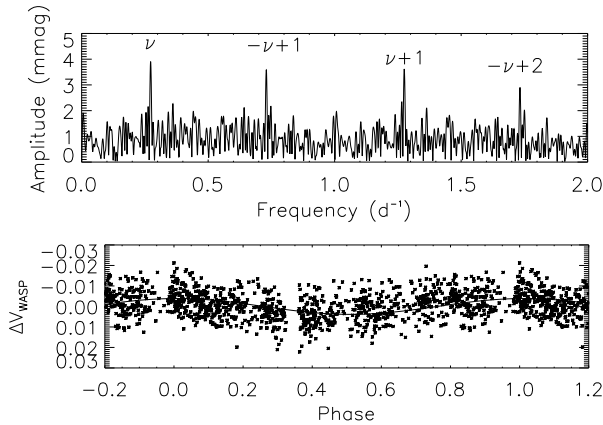
Figure 12. Low frequency periodogram and phase folded lightcurve of J1640. The data are folded on a period of 3.67 d and shown in phase bins of 0.001. The labelled peaks are the true frequency (ν) and the positive and negative aliases.

Figure 13. Periodogram and Shane/HamSpec spectrum of J1844.

4.1.9   J1844

J1844 shows a low amplitude pulsation at 181.73 d^{-1} (Fig. 13). We classify this star as A7p with a $T_{\rm eff}$ of about 7000 K. The spectra for this target were obtained using the Hamilton Echelle Spectrometer mounted on the Shane 3-m telescope at Lick observatory (Fig. 13). We utilised this instrument to gain a high resolution spectrum to be able to perform a full abundance analysis on J1844 as it lies in the *Kepler* field. Identified as KIC 7582608, the target has been observed in LC mode for the duration of the mission. Analysis of both the *Kepler* data and the HamSpec spectrum is under-way (Holdsworth et al., in preparation).

We observe J1844 to have a rotationally modulated lightcurve with a period of 20 d (Fig. 14), a signature which is also present in the *Kepler* data. This is the longest rotation period roAp star we present. The mono-periodic pulsations are similar to those of HD 12098 which pulsates at 189.22 d^{-1} with a blue-band amplitude of 3 mmag (Martinez et al. 2000).

Figure 14. Low frequency periodogram and phase folded lightcurve of J1844. The data are folded on a period of 20.2 d, and are shown in phase bins of 0.001. The labelled peaks are the true frequency (ν) and its harmonic and their positive and negative aliases.

4.1.10   J1940

J1940 shows pulsations at 176.39 d^{-1}, and is the highest amplitude roAp star discovered by SuperWASP at 4.2 mmag (Fig. 15). Given the effects of amplitude reduction of pulsations in the WASP data, J1940 may be the highest amplitude roAp star known. The SALT/RSS classification spectrum was obtained at a low S/N due to the faintness of the target. After smoothing the spectrum (by convolving it with a Gaussian profile), we deduce that J1940 is an F2p star with enhancements of Eu II (Fig. 15). We also detect a low-frequency signal in the photometry with a period of 9.58 d (Fig. 16). J1940 is a prime example of the large pixel sizes of the WASP cameras, and the possible blending that this introduces. Fig. 17 shows an DSS image of the target star (centre) and surrounding objects. The over-plotted circle represents the photometric aperture of WASP (with a radius of 48″). To confirm the source of the high-frequency pulsation, we used the TRAPPIST telescope (Jehin et al. 2011) to observe the target for 3 h. TRAPPIST is a 0.6-m robotic telescope situated at the ESO La Silla Observatory. Backed by a CCD camera of 2048 × 2048 pixels, the instrument achieves a plate scale of 0.6″ per pixel. This vastly superior plate scale compared to WASP, enabled us to confirm that J1940 is the source of the pulsation (Fig. 18). We were, however, unable to confirm the origin of the low frequency signature which may originate on one of the other objects in the aperture.

### 4.2   Other pulsating stars

As we have a lower boundary of 50 d^{-1} as our search criterion, we also anticipated the detection of fast δ Sct systems. In total, we detect 375 objects which have periods less than 30 min. We chose, for follow-up spectroscopic observations, objects which appear to us as either possibly relatively slow roAp stars, with the slowest known being HD 17765 (61 d^{-1}; Alentiev et al. 2012), or multi-periodic δ Sct stars.

Of our spectroscopically observed targets, we classify 13 stars as new pulsating Am stars, with a frequency range of $65-164$ d^{-1}, and temperature range of $7700-8300$ K. How-

Table 5. Abridged version of the photometric information for the δ Sct pulsators. In the full table, available on-line[a], columns 6 − 15 give the first five frequencies, if present, above 50 d^{-1}.

WASP ID	Other ID	V	ν_1 (d^{-1})	A_1 (mmag)	...	ν_5 (d^{-1})	A_5 (mmag)
1SWASPJ000415.12-172529.6	HD 225186	9.05	60.08	3.40	...	–	–
1SWASPJ000537.79+313058.8	TYC 2259-818-1	11.70	52.92	1.47	...	–	–
1SWASPJ000830.50+042818.1	TYC 4-562-1	10.16	150.26	0.76	...	–	–
1SWASPJ000940.84+562218.9	TYC 3660-1935-1	10.34	66.37	3.15	...	–	–
1SWASPJ002436.35+165847.3	HD 2020	8.50	54.41	3.40	...	–	–

[a] Also available at CDS
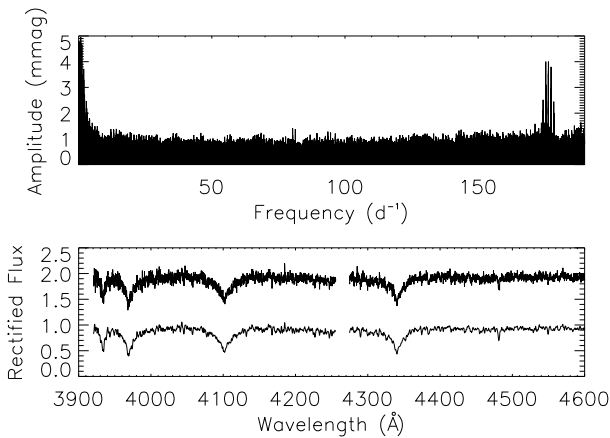
Figure 15. Periodogram and SALT/RSS spectrum of star J1940.
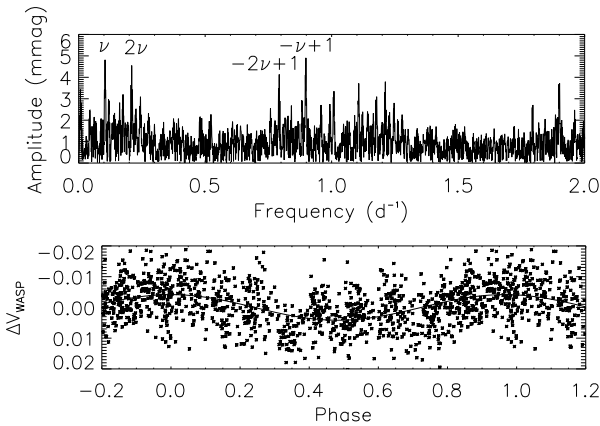
Figure 16. Low frequency periodogram and phase folded lightcurve of J1940. The data are folded on a period of 9.58 d and shown in phase bins of 0.001. The labelled peaks are the true frequency (ν) and its harmonic and their positive and negative aliases.

Figure 17. Photometric aperture (dark circle) for J1940 showing how multiple stars may fall into the aperture. Such targets require follow-up photometry to confirm which object is varying. For this example, TRAPPIST photometry was obtained, confirming the origin of the variations to be the target (central) star. Image from DSS.
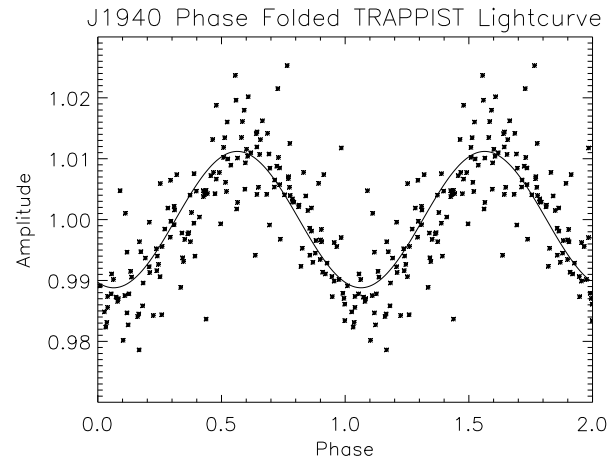
Figure 18. Phase folded TRAPPIST lightcurve for J1940. Obtained to confirm the origin of the variability seen in the WASP data. Data folded on the principal frequency of 176.39 d^{-1}.

ever, we note that at classification resolution there is not always a clear distinction between Am and Ap stars. It is also possible that within this group of stars there are Ap stars which show multi-periodicity of the δ Sct type. Although it was not initially thought that Ap stars pulsate in the δ Sct range, Kurtz (2000) proposed a list of likely targets, with the first example of such a system being HD 21190 (Koen et al. 2001). *Kepler* observations have also detected this phenomenon in 5 of the 7 Ap stars that it has observed (e.g.

Balona et al. 2011a). However, there are currently no known systems which exhibit both high overtone roAp pulsations and low overtone δ Sct pulsations. Theoretical work by Saio (2005) suggests that both high and low overtone p-modes cannot co-exist in magnetic Ap stars as δ Sct pulsations are
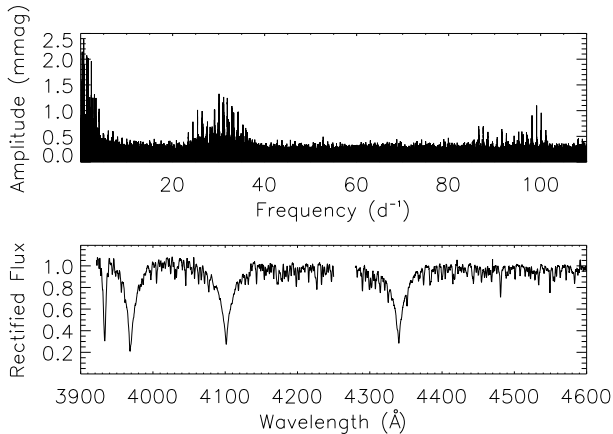
Figure 19. Periodogram and SALT/RSS spectrum of J1403.

Figure 20. Low frequency periodogram and phase folded lightcurve of J1403. The data are folded on a period of 1.5053 d and shown in phase bins of 0.001. The frequency on which the data are folded has a FAP of 0.00. The labelled peaks are the true frequency (ν) and its harmonic and their positive and negative aliases.

suppressed by the presence of the magnetic field, whereas roAp pulsations can be enhanced. However, our survey has identified a few targets, such as J1917 (Section 4.2.2), which show both low and high overtone p-modes in a single target. Further observation are needed, however, to eliminate any other explanations such as target blending and binary systems.

We present below four further targets which show pulsations above 80 d^{-1} for which we have obtained spectra.

The remaining 23 targets for which we obtained spectra are presented in Appendix A. We also provide an on-line catalogue of all the variable systems which show periods shorter than 30 min. Table 5 shows an example of the on-line table format.

4.2.1 J1403

J1403 is an interesting target as our observations show it to pulsate in two distinct frequency ranges (Fig. 19 top). We detect 9 pulsational frequencies between 25 and 34 d^{-1} and 4 between 87 and 100 d^{-1}. We classify the star as A9 (Fig. 19 bottom), however we note different classifications recorded in the literature (e.g. A3/5III; Houk 1978, F0V; Pickles & Depagne 2010, F8 (HD)). We detect low-frequency variations in J1403 at a period of 1.5053 d. The phases folded plot (Fig. 20) shows that this target is most likely an ellipsoidal variable. In such a case, we do not expect this target to be a hybrid pulsator, but a pulsating non-eclipsing binary pair.

4.2.2 J1917

J1917 also shows pulsations in two separate regions. However, here we have pulsations in the δ Sct range (41.3, 45.5 & 53.1 d^{-1}) and a single peak in the higher frequency domain (164 d^{-1}). We obtained a classification spectrum with the RSS spectrograph on SALT, revealing the star to be Am in nature. Similar to the blending problem we saw with J1940, J1917 also has nearby objects which may have caused this multi-periodic lightcurve (Fig. 21). We again used the TRAPPIST telescope to confirm that J1917 is the source of the pulsations (see Fig. 22). The star is listed in the Washington Double Star catalogue (WDS; Mason et al. 2001)
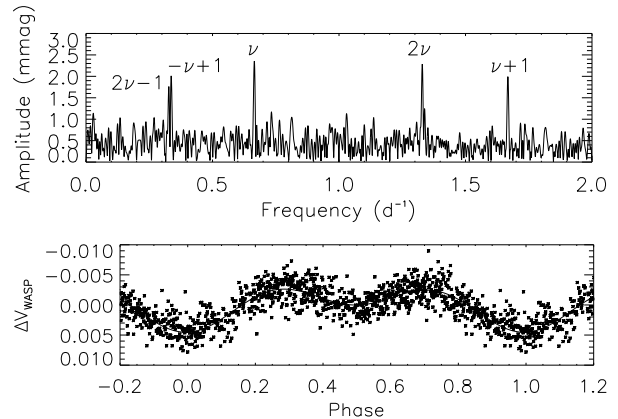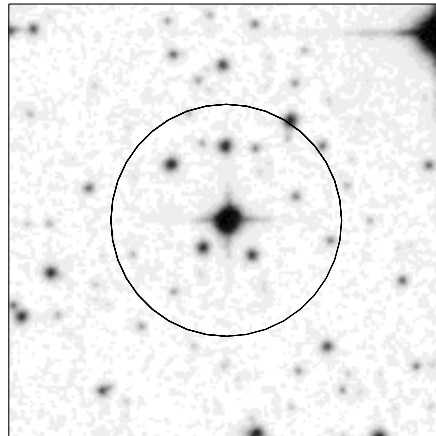

Figure 21. Photometric aperture (dark circle) for J1917 showing multiple stars in the WASP aperture. Follow-up observations using the TRAPPIST telescope confirm the pulsations are originating from the central object. Image from DSS.

with a separation of 1.3″ based on two observations in the 1930s. We estimate the distance to J1917 to be about 400 pc, which suggests a binary separation of 500 au. The two components of the visual binary system have magnitudes of 10.8 and 14 in the *V*-band (Mason et al. 2001). If the companion is a main-sequence star, given the spectral type of the primary, we estimate it to be a G-type star. We would expect none of the pulsations to originate from a G star. We propose that either both sets of pulsations originate on the Am star, or that there is an unresolved binary system with two pulsating components. Further observations are required to fully understand the nature of J1917.

4.2.3 J2054

J2054 shows two pulsations over 100 d^{-1}. The strongest is at 104.86 d^{-1} with an amplitude of 1.1 mmag, with the second at 100.44 d^{-1} with an amplitude of 0.53 mmag. The
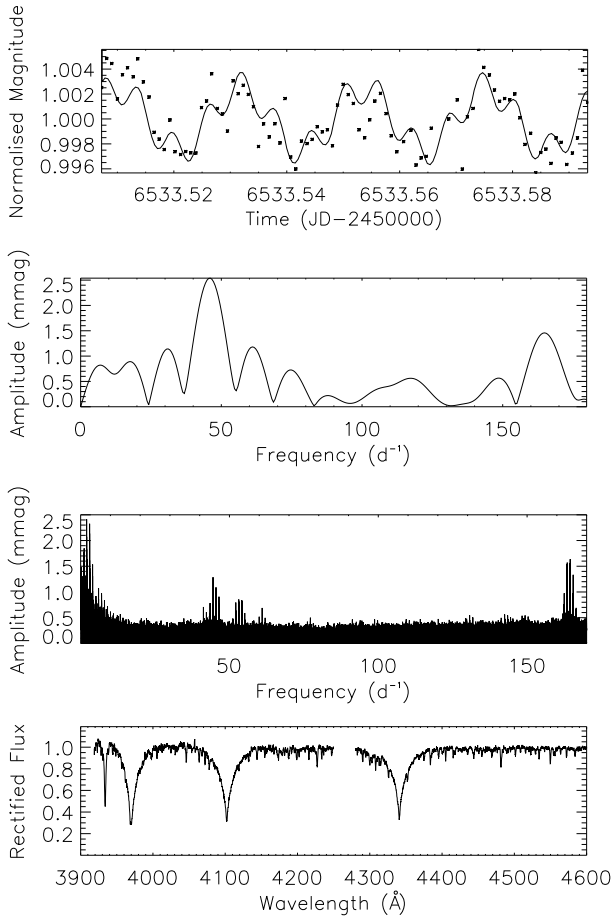
Figure 22. Top: Two hours of TRAPPIST follow-up observations confirm the pulsations originate on J1917 (the data have been binned on ~ 1 min intervals). Second: Periodogram of the TRAPPIST data. The peak at 45 d^{-1} is stronger than in the WASP periodogram as there are many pulsations contributing power that are not resolved in just 2 h. The high-frequency is at about the same amplitude as the WASP data. Third: The WASP periodogram of J1917 for comparison. Bottom: SALT/RSS spectrum of J1917 showing it to be an A7m star.

Shane/HamSpec spectrum obtained for this target indicates that it is an A3m: star based on a weakened Ca K line and slightly enhanced Sr. We note that there is no clear depletion of Sc II. We estimate a $v \sin i$ of ~ 50 km s^{-1} for J2054.

Low frequency variations are noted in the photometry, corresponding to a period of 1.3 d (Fig. 24). When the data are folded on this period, the resulting phase diagram shows two maxima with unequal minima. The lightcurve indicates a binary target, where the pulsations may originate in one or both components. However there is no evidence for this in the single spectrum we obtained.

J2054 is the fastest Am star that we have found with SuperWASP, superseding the previous fastest, HD 108452 (Smalley et al. 2011) pulsating at 71 d^{-1}. Our results have therefore pushed the boundary of the pulsating Am stars farther into the domain of the roAp stars, further blurring the distinction between these two types of pulsator.
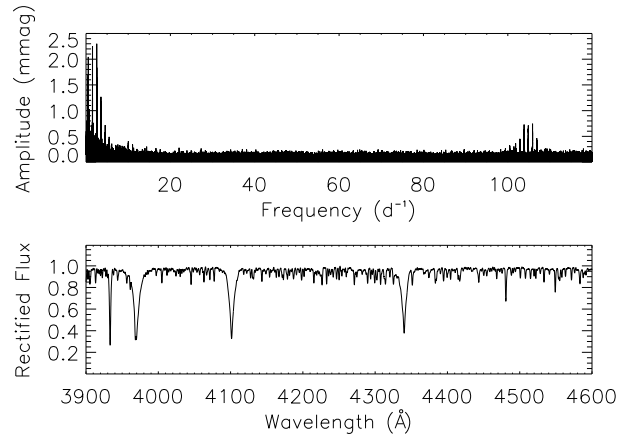
Figure 23. Periodogram and Shane/HamSpec spectrum of J2054.
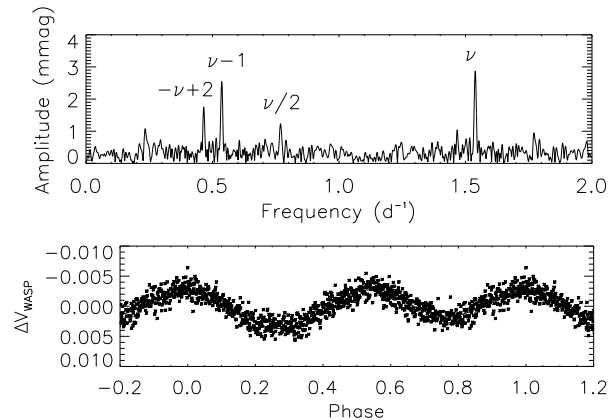
Figure 24. Low frequency periodogram and phase folded lightcurve of J2054. The data are folded on a period of 1.3 d and shown in phase bins of 0.001. The frequency on which the data are folded has a FAP of 0.00. The labelled peaks are the true frequency (ν) and its subharmonic and their positive and negative aliases.

4.2.4 J2305

J2305 is a double-mode, high-frequency Am pulsating star similar in nature to J2054. It pulsates slightly slower than J2054 at 92.75 and 101.68 d^{-1} (Fig. 25 top). We classify J2035 as an A7m star (Fig. 25 bottom).

We detect no low-frequency variability in the Super-WASP photometry, indicating that both pulsations are most likely originating in J2305. Multiple periods have previously been observed in Am stars (e.g. Joshi et al. 2003; Balona et al. 2011b), however not at the frequencies or amplitudes presented here.

5 CONCLUSION

We have exploited the SuperWASP archive in the search for rapidly varying F-, A- and B-type stars. Our survey, of over 1.5 million objects, has resulted in the discovery of 10 new roAp stars as well as 13 new pulsating Am stars. Further to
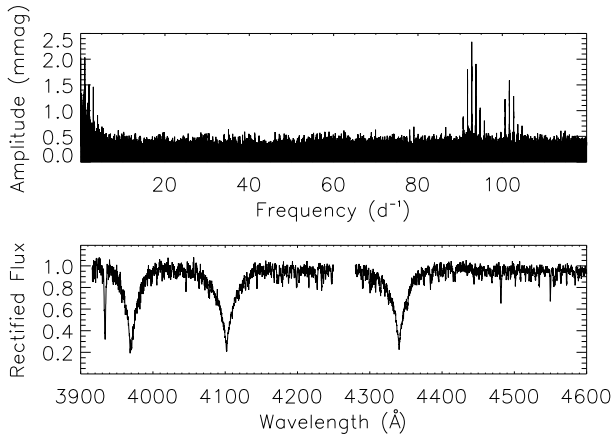
Figure 25. Periodogram and SALT/RSS spectrum of J2305.

this, there are over 350 systems which show variations on periods less than 30 min.

The discovery of this number of new roAp stars increases the known stars of this class by 20 per cent, providing a larger sample for further study.

This work shows the power of photometric surveys to identify a whole variety of variable stars. There are many more sources of data that can be exploited in a similar way to that which we have presented here for the search for rare and interesting pulsating stars. We have been able to push the previous limits of pulsation frequencies in some types of A stars, leading to a greater frequency overlap between different pulsator classes.

REFERENCES

Aerts C., Christensen-Dalsgaard J., Kurtz D.W., 2010, Asteroseismology, Springer

Alentiev D., Kochukhov O., Ryabchikova T., Cunha M., Tsymbal V., Weiss W., 2012, MNRAS, 421, L82

Amado P.J., Moya A., Suárez J.C., Martín-Ruiz S., Garrido R., Rodríguez E., Catala C., Goupil M.J., 2004, MNRAS, 352, L11

Bakos G., Noyes R.W., Kovács G., Stanek K.Z., Sasselov D.D., Domsa I., 2004, PASP, 116, 266

Balmforth N.J., Cunha M.S., Dolez N., Gough D.O., Vauclair S., 2001, MNRAS, 323, 362

Balona L.A., Zima W., 2002, MNRAS, 336, 873

Balona L.A. et al., 2011a, MNRAS, 410, 517

Balona L.A. et al., 2011b, MNRAS, 414, 792

Bevington P.R., 1969, Data reduction and error analysis for the physical sciences, New York: McGraw-Hill

Borucki W.J. et al., 2010, Science, 327, 977

Breger M., 1970, ApJ, 162, 597

Breger M., et al., 1993, A&A, 271, 482

Catanzaro G. et al., 2011, MNRAS, 411, 1167

Conti P.S., 1970, PASP, 82, 781

Debosscher J., Blomme J., Aerts C., De Ridder J., 2011, A&A, 529, A89

Droege T.F., Richmond M.W., Sallman M.P., Creager R.P., 2006, PASP, 118, 1666

Elkin V., Kurtz D.W., Mathys G., 2008, Contr. Astron. Observ. Skalnate Pleso, 38, 317

Evans D.W., Irwin M.J., Helmer L., 2002, A&A, 395, 347

Fouqué P. et al., 2000, A&AS, 141, 313

Gautschy A., Saio H., 1998, in Deubner F.L., Christensen-Dalsgaard J., Kurtz D.W., eds, Proc IAU Symp. 185, New Eyes to See Inside the Sun and Stars, Kyoto, Japan, p. 277

Gilliland R.L. et al., 2010, ApJL, 713, L160

Gray R.O., Corbally C.J., 2009, Stellar Spectral Classification. Princeton Univ. Press. Princeton, NJ

Grigahcène A. et al., 2010, ApJL, 713, L192

Høg E. et al., 1997, A&A, 323, L57

Houk N., 1978, Michigan catalogue of two-dimensional spectral types for the HD stars, University Microfilms International

Huber P.J., 1981, Robust Statistics, Wiley

Jehin E. et al., 2011, The Messenger, 145, 2

Joshi S. et al., 2003, MNRAS, 344, 431

Koch D.G. et al., 2010, ApJL, 713, L79

Kochukhov O., 2003, A&A, 404, 669

Kochukhov O., Alentiev D., Ryabchikova T., Boyko S., Cunha M., Tsymbal V., Weiss W., 2013, MNRAS, 431, 2808

Koen C., Kurtz D.W., Gray R.O., Kilkenny D., Handler G., Van Wyk F., Marang F., Winkler H., 2001, MNRAS, 326, 387

Koen C., 2010, Ap & SS, 329, 267

Kreidl T. J., 1990, Inf. Bull. Var. Stars, 3539, 1

Kurtz D.W., 1981, Inf. Bull. Var. Stars, 1915, 1

Kurtz D.W., 1982, MNRAS, 200, 807

Kurtz D.W., 1989, MNRAS, 238, 1077

Kurtz D.W., 1990, ARA&A, 28, 607

Kurtz D.W., 2000, in Brege M., Montgomery M.H., eds, ASP Conf. Ser. Vol. 210, Delta Scuti and Related Stars.

Astron. Soc. Pac., San Francisco, p. 287

Kurtz D.W., Martinez P., 1993, Inf. Bull. Var. Stars, 3966, 1

Kurtz D.W. et al., 2011, MNRAS, 414, 2550

Kurucz R.L., 1993, Kurucz CD-ROM 13. SAO, Cambridge, USA

Lenz P., Breger M., 2005 CoAst, 146, 53

Martinez P., Kurtz D.W., 1990, Inf. Bull. Var. Stars, 3510, 1

Martinez P., Kurtz D.W., 1994, MNRAS, 271, 118

Martinez P. et al., 2000, Inf. Bull. Var. Stars 4853, 1

Mason B.D., Wycoff G.L., Hartkop, W.I., Douglass G.G., Worley C.E., AJ, 122, 3466

Maxted P.F.L. et al., 2011, PASP, 123, 547

Monet D.G. et al., 2003, AJ, 125, 984

Norton A.J. et al., 2011, A&A, 528, A90

Pickles A., Depagne É., 2010, PASP, 122, 1437

Pojmański G., 1997, AcA, 47, 467

Pollacco D.L. et al., 2006, PASP, 118, 1407

Press W.H., Rybicki G.B., 1989, ApJ, 338, 277

Press W.H., Teukolsky S.A., Vetterling W.T., Flannery B.P., 1992, Numerical recipes in FORTRAN. The art of scientific computing, Cambridge University Press

Paunzen E., Netopil M., Rode-Paunzen M., Handler G., Božić H., Ruždjak D., Sudar D., 2012, A&A, 542, A89

Reegen P., 2007, A&A, 467, 1353

Renson P., Manfroid J., 2009, A&A, 498, 961

Rusomarov N. et al., 2013, A&A, 558, A8

Saio H., 2005, MNRAS, 360, 1022

Skrutskie M.F. et al., 2006, AJ, 131, 1163

Smalley B. et al., 2011, A&A, 535, A3

Smalley B., 2013, in Chaplin W., Guzik J., Handler G., Pigulski A., eds, Proc IAU Symp. 301, Precision Astero-seismology, in press

Smalley B., Smith K.C., Dworetsky M.M. 2001. UCLSYN User Guide `http://www.astro.keele.ac.uk/~bs/publs/uclsyn.pdf`

Smith M.A., 1973, ApJS, 25, 277

Stibbs D.W.N., 1950, MNRAS, 110, 395

Stoehr F. et al., 2008, in Argyle, R.W., Bunclark, P.S., Lewis, J.R. eds, ASP Conf. Ser. Vol. 394, Astronomical Data Analysis Software and Systems XVII. Astron. Soc. Pac., San Francisco, p. 505

Tamuz O., Mazeh T., Zucker S., 2005, MNRAS, 356, 1466

Udalski A., Szymanski M., Kaluzny J., Kubiak M., Mateo M., 1992, AcA, 42, 253

Vogt S.S., 1987, PASP, 99, 1214

Wolff S.C., 1968, PASP, 80, 281

APPENDIX A: SPECTROSCOPICALLY OBSERVED TARGETS

Below we present the periodograms and spectra for the remaining 23 spectroscopically observed targets.
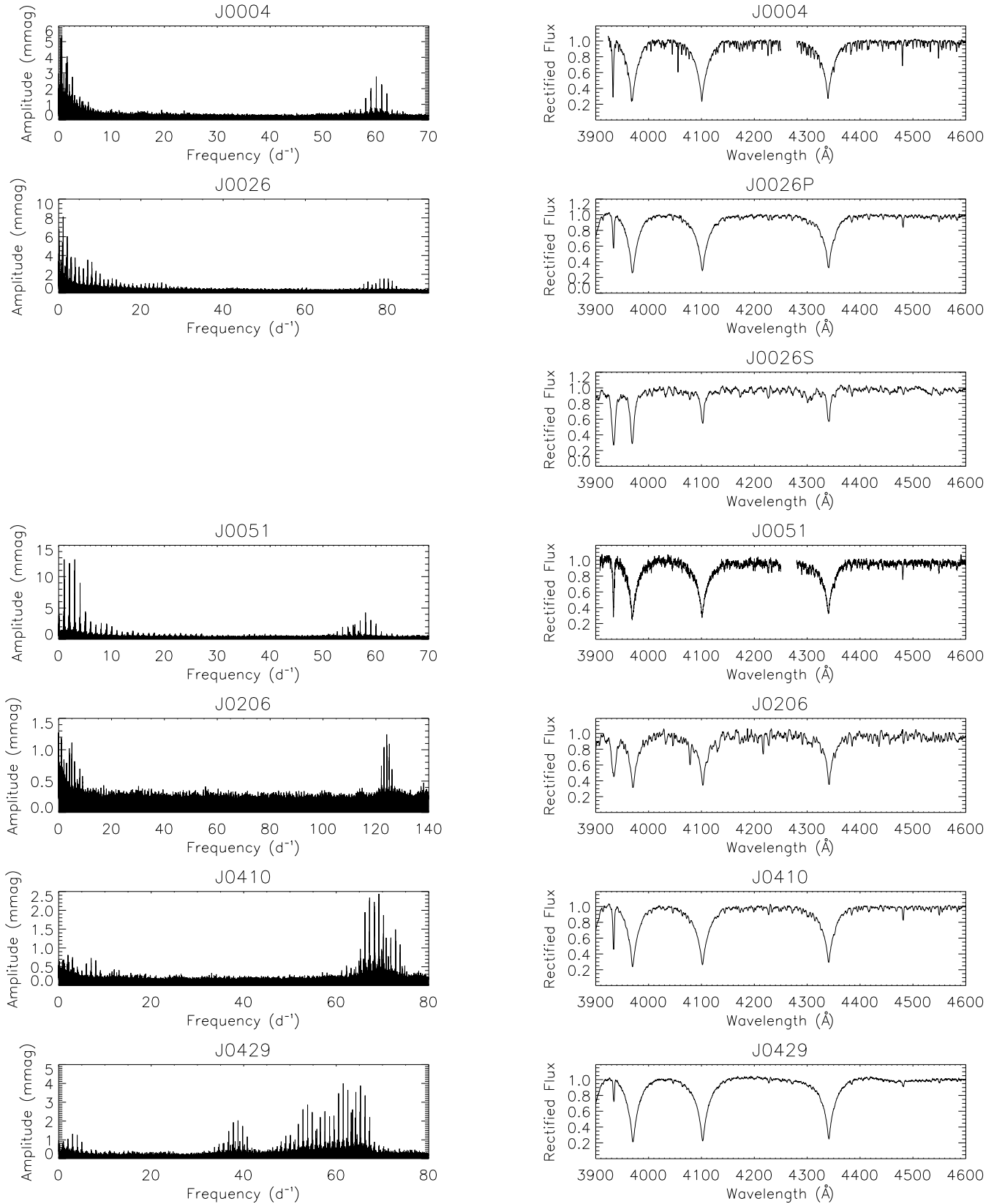
Figure A1. Periodograms and spectra for the remaining spectroscopically observed targets.
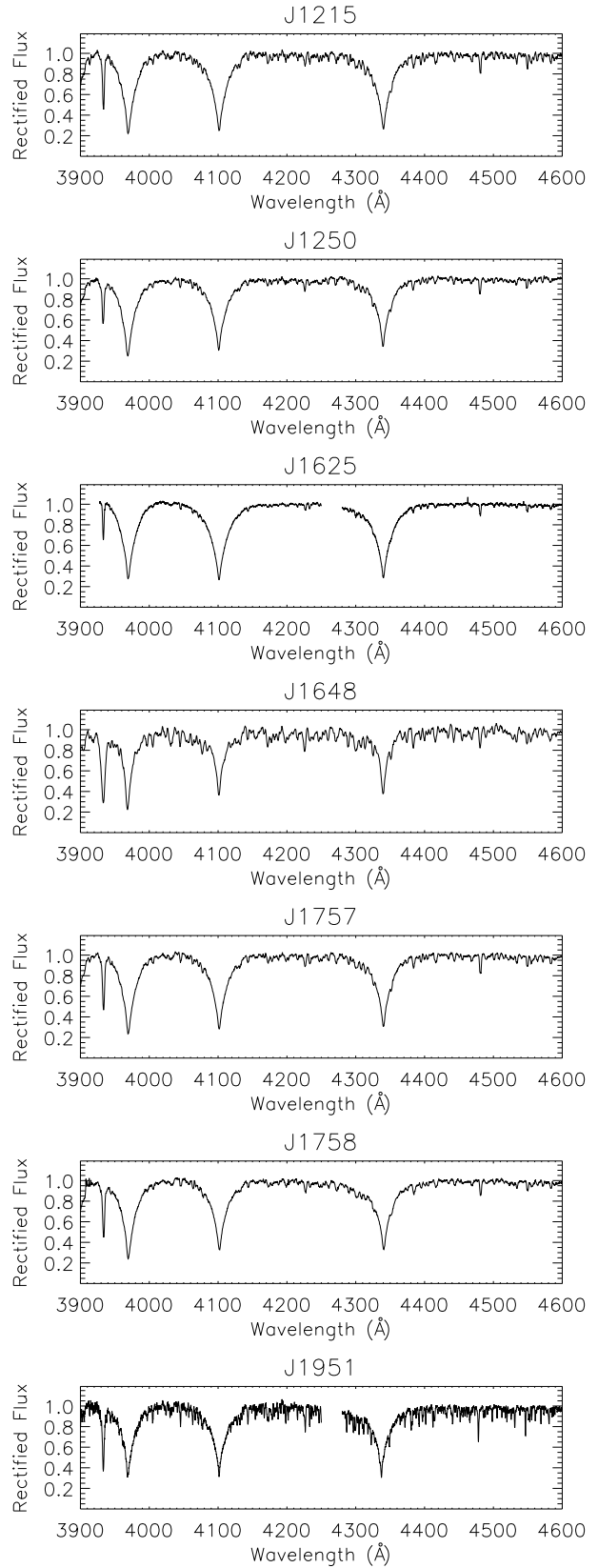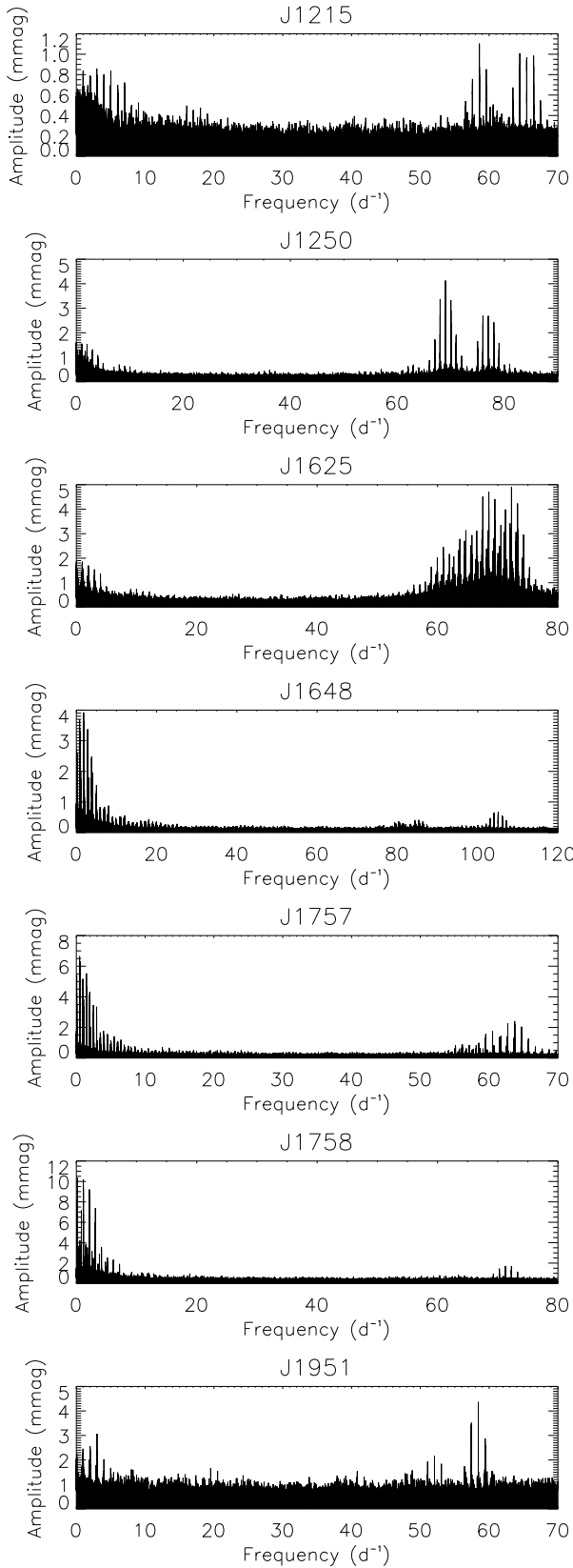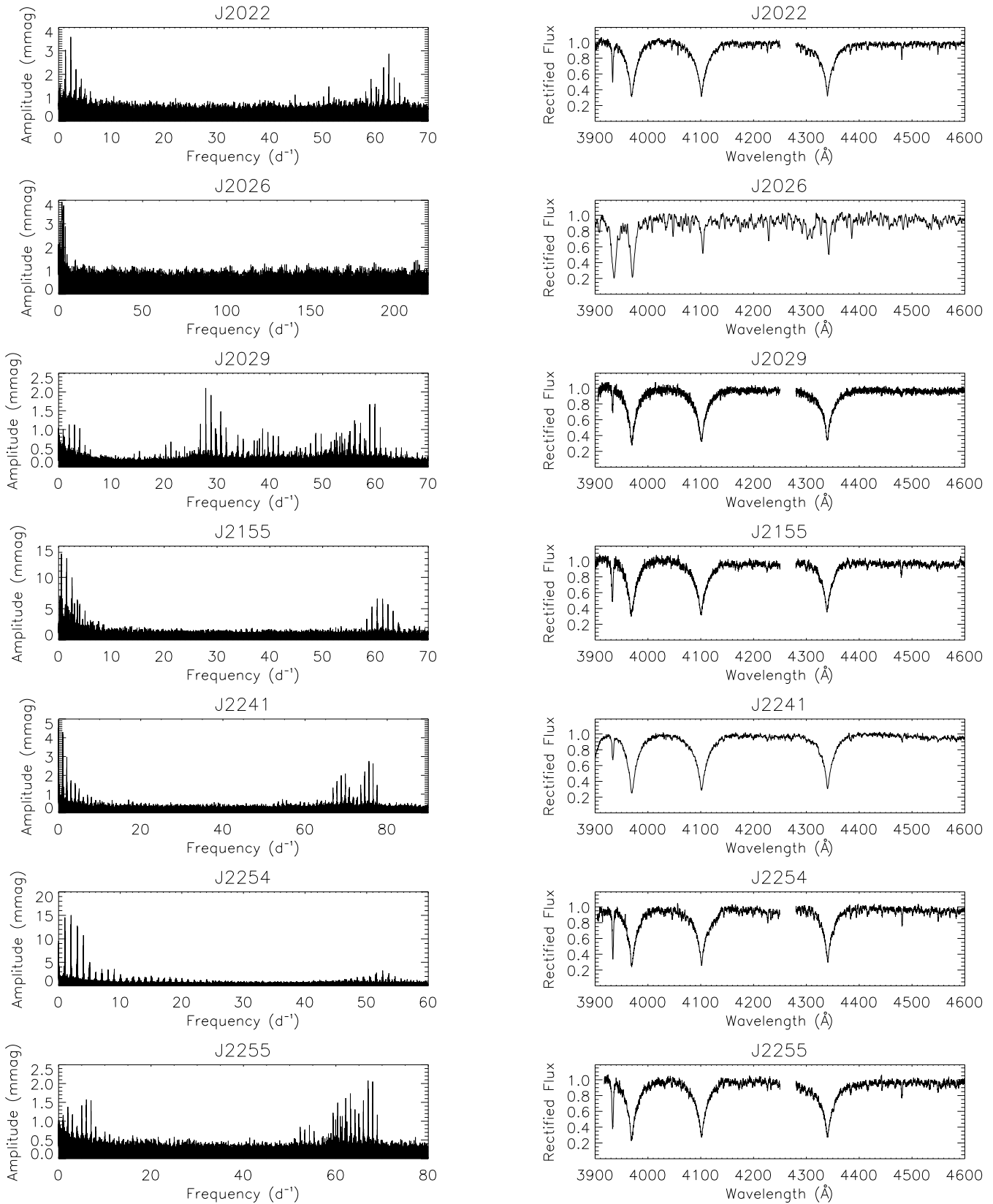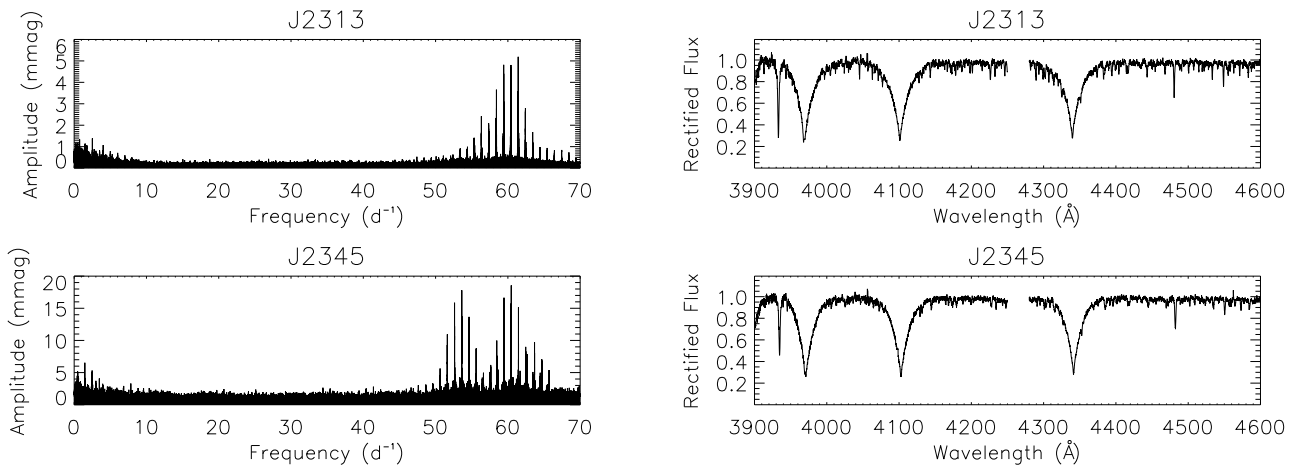
Figure A1. Continued.

Figure A1. Continued.

Figure A1. Continued.